A Novel Rat Model of Dry Eye Induced by Aerosol Exposure of Particulate Matter

Ning Mu,[1,2,*] He Wang,[2,*] Dongyan Chen,[2] Fan Wang,[2] Ling Ji,[2] Can Zhang,[2] Mingxin Li,[2] and Peirong Lu[1]

[1]Department of Ophthalmology, the First Affiliated Hospital of Soochow University, Suzhou, , Jiangsu Province, P.R. China
[2]Department of Ophthalmology, the Affiliated Hospital of XuZhou Medical University, Xuzhou, Jiangsu Province, P.R. China

Correspondence: Peirong Lu, Department of Ophthalmology, the First Affiliated Hospital of Soochow University, Shizi Street 188, Suzhou, 215006, Jiangsu Province, P.R. China; lupeirong@suda.edu.cn.
Mingxin Li, Department of Ophthalmology, the Affiliated Hospital of XuZhou Medical University, Huai Hai West Street 99, Xuzhou, 221000, Jiangsu Province, P.R. China; lmx216@vip.sina.com.

NM and HW contributed equally to the work presented here and should therefore be regarded as equivalent authors.

Received: May 20, 2021
Accepted: December 30, 2021
Published: January 28, 2022

Citation: Mu N, Wang H, Chen D, et al. A novel rat model of dry eye induced by aerosol exposure of particulate matter. *Invest Ophthalmol Vis Sci.* 2022;63(1):39. https://doi.org/10.1167/iovs.63.1.39

Purpose. The purpose of this study was to introduce a novel dry eye rat model induced by aerosol exposure of particulate matter (PM).

Methods. A total of 30 female Sprague Dawley (SD) rats divided into 3 groups: the control group, the low-level exposed group, and the high-level exposed group. The rats in the experience groups were directly exposed to PM samples in the exposure chamber over 14 days. The clinical observation, including tear volume, corneal fluorescein staining, breakup time (BUT), inflammation index, corneal irregularity score, and corneal confocal microscopy. Eyeballs were collected on day 14 for hematoxylin and eosin (H&E) staining and PAS staining. TUNEL assay, CD45, and Ki67 immunostaining was performed and corneal ultrastructural changes were detected by electron microscopy. IL-1β, TNF-α, IFN-γ, and NF-κB Western blot analysis were used to observe the possible pathogenesis.

Results. In the PM-treated groups, the number of layers in the corneal epithelium and corneal nerve fiber length were significantly decreased compared with that of the control group. The number of corneal epithelial microvilli and chondriosome/desmosomes were drastically reduced in PM-treated groups. Confocal microscopy and CD45 immunohistochemistry showed inflammatory cell infiltration in the PM-treated groups. PM caused apoptosis of corneal and conjunctival epithelial cells while leading to abnormal epithelial cell proliferation, meanwhile, conjunctival goblet cells in the PM-treated group were also significantly reduced. PM significantly increased the levels of IL-1β, TNF-α, IFN-γ, and p-NF-κB-p65 in the cornea.

Conclusions. Aerosol exposure of PM can reduce the stability of tear film and cause the change of ocular surface, which is similar to the performance of human dry eye, suggesting a novel animal model of dry eye.

Keywords: particulate matter, ocular surface, dry eye, animal model

According to the Tear Film and Ocular Surface Society (TFOS) International Dry Eye Workshop (DEWS) II 2017,[1] dry eye is a multifactorial cause of decreased tear film stability. Dry eye is the most common ocular surface disease affecting vision and quality of life. The common symptoms of dry eye include dry and astringent eyes, foreign body sensation, burning sensation, itching, pain, redness, asthenopia, blurred vision, vision fluctuation, etc. Severe dry eye can lead to corneal ulcer, decreased vision, and even blindness.[2]

There are many factors that can cause dry eye, such as wearing contact lenses, refractive surgery, long-term exposure to video terminals, systemic diseases (such as Sjogren's syndrome, diabetes, and systemic lupus erythematosus),[3,4] etc. in addition, environmental factors are also important causes of dry eyes.[5,6] The increasing environmental pollution is a great challenge in the process of industrialization, especially in developing countries. The impact of environmental pollution on human health has attracted more and more attention of the public, and there are many studies on it.[7,8]

Particulate matter (PM) is a heterogeneous mixture of inorganic salts and organic compounds, such as polycyclic aromatic hydrocarbons (PAHs), heavy metals, nitrogen oxides, carbon oxides, and chlorinated pesticides.[9] In 2013, PM was defined as a class I carcinogen by the World Health Organization (WHO). PM may be a risk to human health by causing respiratory diseases,[10,11] skin diseases,[12] ischemic cardiovascular events,[13,14] and metabolic diseases.[15,16]

Eyes are exposed to external environment, so they are directly affected by PM. The PM exposure can reduce tear film stability, inflammation, and oxidative stress, resulting in multifactorial damage of corneal epithelial cells.[17] Many studies have attempted to understand the relationship between PM and dry eye, one of them, through a time-stratified case cross study, provides evidence that the number of visits of patients with dry eye is significantly related to the concentration of air pollutants in Hangzhou, China.[18] Some studies have reported that cell damage can be observed by adding PM to cultured corneal epithelial cell lines.[19–21] In the study of diesel exhaust, researchers not only

Copyright 2022 The Authors

This work is licensed under a Creative Commons Attribution-NonCommercial-NoDerivatives 4.0 International License.

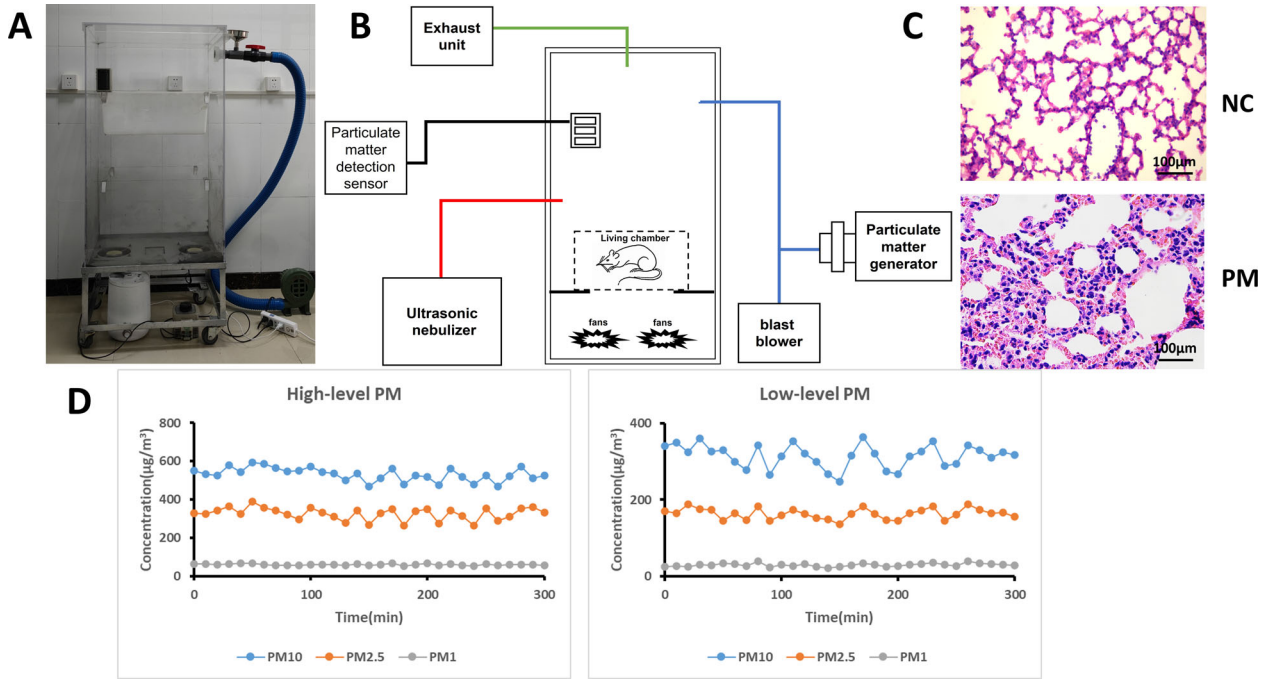

Figure 1. Aerosol exposure system. (**A**) The photograph of the aerosol exposure system. (**B**) The schematic of the aerosol exposure system. (**C**) Histopathological sections and H&E staining of rat lungs. Compared with the control group, a large number of inflammatory cell infiltrates were observed in the lungs of PM treated rats. Scale bar: 100 μm. (**D**) Representative graph for the high or low concentration of PM in the exposure chamber over 5 hours. PM10, PM with an aerodynamic diameter ≤10 μm; PM2.5, PM with an aerodynamic diameter ≤2.5 μm; PM1, PM with an aerodynamic diameter ≤1 μm.

observed the toxicity of diesel exhaust on corneal epithelial cells cultured in vitro, but also confirmed that it can affect the stability of ocular surface structure in a mouse model.[22,23] Some scholars try to use PM topical eye drops to observe its effect on the ocular surface.[24,25] Although this local exposure method induces dry eyes, this method still has limitations because it cannot reflect the concentration level and action mode of PM in the atmospheric environment. Recently, there is a paper on the effect of PM-exposure on dry eye in the atmosphere.[26] However, the instruments used only expose animal heads, restrict the activity and normal behavior of animals, and cannot completely simulate the characteristics of ocular surface damage caused by air pollution. The research contents are relatively simple, and no molecular mechanism is involved. In order to overcome these limitations, we designed a PM aerosol atomization system in which the experimental animals can live in it for a long time, so as to simulate the influence of PM level on the stability of eye surface and tear film in a real environment.

Materials and Methods

Aerosol PM Exposure System

PM samples were provided by the Xuzhou Environmental Monitoring Station. During November 1 to 31, 2020, a super station at Xuzhou City acquired total suspended particulates (TSPs) using the TH-16A 4-channel atmospheric particulate automatic sampler (Model: MF16-1600-18; Nanjing Wimet Scientific Instrument Co. Ltd.) and filtered them through Whatman PTFE membranes. Samples were collected continuously for 22 hours from 10:00 AM to 8:00 AM the next day. The PTFE membrane containing PM sample was cut into 1-cm × 1-cm pieces and immersed in distilled water for 10 minutes, and then ultrasonically vibrated for 45 minutes to separate the sample from the PTEE membrane. The sample was filtered by 6 layers of gauze and then dried in vacuum, weighed, and stored at 4°C.[27]

The Aerosol PM exposure system has been widely used for investigating the biological effects of PM, including lung injury,[28] cardio-cerebrovascular injury,[29] and isolated cells.[30] In short, the system consists of ultrasonic atomizer, PM container, PM exposure chamber, PM detection sensor, blower and exhaust gas recovery device (Figs. 1A, 1B). In this study, we maintained the temperature of PM exposure chamber at 22–24°C suitable for rat survival. Due to the humidification effect of the atomization device, the humidity of PM exposure chambers was high and had been measured to be approximately between 60% and 80%. The air velocity of blower was consistently maintained at 5 L min^{-1} in traditional single pneumatic atomization for proper functioning. Hematoxylin-eosin (HE) staining results of lung histopathological sections showed that after PM exposure, the lungs of rats exhibited inflammatory cell infiltration, widened tissue gaps, and visible particulate matter deposition, suggesting the occurrence of PM-related lung injury (Fig. 1C).

The air quality guidelines of WHO point out that living in a PM below 50 μg/m^3 (24-hour average) can effectively reduce PM-related health risks.[31] However, PM concentrations in some parts of China are much higher than 50 μg/m^3. According to the air quality standard issued by the Ministry of Environment of the People's Republic of China, the 24-hour concentration limit of TSP matter is 300 μg/m^3, exceeding this standard is called severe pollution. However, the average concentration of PM in Beijing during spring of 2018 exceeded 500 μg/m^3.[32] Based on these reports, we exposed animals to a low-level of 300 μg/m^3 and high-level of 500 μg/m^3 in the aerosol exposure system chamber to

test the suitability of the experimental setup to study dry eye syndrome (DES) in vivo. The mean concentration of PM10, PM2.5, and PM1 in the system of low-level was 349 ± 23.6, 176 ± 16.2, and 35 ± 7.8 μg/m^3, whereas high-level was 564 ± 10.6, 328 ± 13.2, and 55 ± 5.7 μg/m^3 during exposure, respectively (Fig. 1D).

Animal Experimental Procedure

Totally, 30 female specific pathogens free (SPF) Sprague Dawley rats (6 weeks old, 150–200 g) purchased from Laboratory Animal Center of Xuzhou Medical University were used for this study. No abnormality was found in the anterior segment and fundus when examined with slit lamp microscope and fundus examination. The results for the Schirmer I test (SIT) were ≥10 mm/5 minutes. All procedures were performed in accordance with the ARVO Statement for the Use of Animals in Ophthalmic and Vision Research and were approved by the animal ethics committee of Xuzhou Medical University (Xuzhou, China).

After one 1-week acclimatization period, rats were randomly divided into 3 groups: the control group (n = 10), the low-level exposed group (n = 10), and the high-level exposed group (n = 10). DES was induced by PM samples using an aerosol exposure system according to a modified procedure.[33] Briefly, to induce DES, rats were directly exposed to different concentrations of PM samples in the exposure chamber for 5 hours per day over 14 days, as shown in Figures 1A, B, and C. Following a 14-day exposure, rats were measured for corneal irregularity score, confocal corneal microscopy, corneal fluorescein score, tear breakup time (BUT), tear volume, and inflammatory index. Following euthanasia, the eyes were collected, in which inflammation, proliferation, apoptosis, and electron microscope, as well as the number of goblet cells were assessed.

Tear Volume, Fluorescein and BUT Measurement

Tear volume, fluorescein, and BUT measurement was done as previously described.[34] All tests were carried out in the same darkroom with the same operator under the same slit lamp brightness. The volume of tear secretion was measured by phenol red cotton thread (FCI Ophthalmics, Pembrooke, MA, USA) test on days 0, 4, 7, 10, and 14 post-treatments. In brief, the basic tear secretion of rats in each group was measured at the same time point. We fixed the head and gently pulled down the eyelids to expose the conjunctival sac. The phenol red cotton thread was bent 5 mm and placed under 1/3 conjunctival sac. After 15 seconds, the line was drawn out and the length of the red line was measured. We repeated the measurement for three times in each eye and took the average value. At the end of the test, the eyes were closed to avoid overexposure and ocular surface irritation. Fluorescent staining: 5 uL of 0.1% sodium fluorescein staining solution was applied to the eye surface of rats, and the damage site of the eye surface was observed by cobalt blue light under slit lamp microscope. For BUT, after the fluorescein sodium staining, the rats were forced to close their eyes, and then the upper and lower eyelids of the rats were separated under slit lamp. The corneal surface was carefully observed with low brightness cobalt blue light to find the first black hole of the complete tear film, and the time was recorded. We repeated the test for three times and took the average value.[35] The standard of corneal fluorescein staining was as follows: 0 = no staining; 1 point = slight spot staining, less than 30 spots; 2 points = dot staining more than 30 spots, without diffuse staining; 3 points = severe diffuse staining, but no plaque; and 4 points = plaque staining.

Corneal Irregularity Score

After 14 days of PM treatment, the ocular surface of rats was photographed with a stereomicroscope (DED1L; Kanghua, Chongqing, China) equipped with oracido ring. The criteria of corneal irregularity were as follows: no distortion; 1 = the distortion is in a quadrant; 2 = the distortion of two quadrants; 3 = three quadrant distortions; 4 = distortion of all four quadrants; and 5 = severe deformation, unable to identify any ring structure.

In Vivo Confocal Microscopy

A laser scanning confocal microscope (Heidelberg Retina Tomograph [HRT] III/Rostock Cornea Module (RCM), Heidelberg Engineering GmbH, Heidelberg, Germany) was used to examine corneas in vivo. Images covered an area of 400 × 400 μm, with a transversal optical resolution of 1 μm (Heidelberg Engineering). The entire corneal surface was examined; the x-y position and the depth of the optical section were manually controlled using a handle technique adapted to animal eyes. The number of corneal epithelial cells, corneal nerve fiber length (CNFL), corneal inflammatory cells, and corneal endothelial cells were analyzed using Image J (National Institutes of Health, Bethesda, MD, USA), as previously described.[36,37]

Evaluation of Inflammation Level

At 0, 4, 7, 10, and 14 days after PM treatment, the inflammation of rat ocular surface was observed by slit lamp.[38] The inflammatory index score was calculated as follows: ciliary hyperemia (0 = none; 1 = less than 1 mm; 2 = 1 and 2 mm; and 3 = more than 2 mm); central corneal edema (0 = none; 1 = iris details can be seen; 2 = the details of the iris are unclear, but the pupil is visible; and 3 = the pupil is indistinct); and peripheral corneal edema (0 = none; 1 = there are visible iris details; 2 = no iris details visible; and 3 = no visible iris).

Periodic Acid Schiff and Hematoxylin and Eosin Staining

On the 14th day of treatment, the whole eyeball, including the upper and lower conjunctiva, was enucleated out and fixed overnight with 4% paraformaldehyde. The eyeball was embedded with automatic paraffin embedding machine, sectioned with 4 μm thickness, and stained with PAS (Sigma-Aldrich, St. Louis, MO, USA) and H&E after gradient alcohol dewaxing. Three representative slices were selected from the same location for each sample, with four samples in each group. The goblet cell density was determined by calculating the number of PAS positive cells in four different parts of each section and taking the average value.[39]

Terminal Deoxynucleotidyl Transferase Mediated dUTP Biotin Nick end Labeling

TUNEL was used to detect apoptosis with a published method.[40] There were five samples in each group. Three representative sections were selected from the homologous position of each sample. The negative control was the section without biotinylated dUTP.

Investigative Ophthalmology & Visual Science

Immunofluorescent Staining of Ki67 and CD45

Immunodetection of Ki67 and CD45 was performed as described previously.[41] Rabbit anti-rat Ki67 antibody (Servicebio, GB111141, Wuhan, China) at a 1: 800 dilution, and Rabbit anti-rat CD45 antibody (Servicebio, GB113886) at a 1: 300 dilution was used as the primary antibody, followed by incubation with ALEXA fluorophore-conjugated secondary antibodies (Invitrogen, USA) and counterstaining with Hoechst 33342 dye (0.5 g/mL; Invitrogen, USA). Images were obtained using a fluorescence microscope (Nikon, Japan).

Transmission Electron Microscopy

The samples were taken according to the standard processing method of electron microscope.[42] The cornea was cut off along the limbus after the eyeball was removed, the corneal tissue was cut into 1 mm × 2 mm slices with a sharp blade, and then fixed in PBS (pH = 7.4) containing 2.5% glutaraldehyde and 4% paraformaldehyde for 2 hours. Transmission electron microscopy (TEM) images were photographed with a TEM microscope (HT7800; HITACHI, Tokyo, Japan).

Western Blotting Analysis

The removed corneal tissues were lysed with cold RIPA buffer and electrophoresed on 8% SDS-PAGE gels following standard protocols for Western blotting analysis. The following primary antibodies were used: IL-1β (1: 1000; Proteintech, 16806-1-AP, Rosemont, USA), TNF-α (1: 600; Proteintech, 17590-1-AP), IFN-γ (1: 800; Proteintech, 15365-1-AP), NF-κB p65 (phospho S536; 1: 1000; Proteintech, 39691), NF-κB (1: 3000; Proteintech, 66535-1-Ig), and β-actin (1: 10,000; Proteintech, 66009-1-Ig) was used as a loading control. HRP-conjugated goat anti-rabbit IgG (1: 10,000; Proteintech, B900210) was used as the secondary antibody.

Image Processing and Statistical Analysis

Images were processed using Image-Pro Plus 6.0 software (GraphPad Prism, Inc., La Jolla, CA, USA). Two-way ANOVA analysis was performed for comparisons between groups using the SPSS 26.0.0 (SPSS, Chicago, IL, USA). Any $P < 0.05$ was considered statistically significant. Data were represented as mean ± standard error.

Results

Effects of PM on Ocular Surface

According to the results of pre-experimental, in the aerosol exposure system, application of PM at low-level of 300 μg/m^3 and high-level of 500 μg/m^3 5 hours per day for 14 days was determined as the optimal procedure for the induction of DES in the rats. When the concentration of PM was higher than 500 μg/m^3, the respiratory symptoms of rats were aggravated and the mortality was increased, whereas when the PM concentration is lower than 300 μg/m^3 no obvious effects to the eyes were exhibited (data not shown).

Stability of Tear Film and Epithelium Damage

The effect of PM on the cornea was assessed by recording the corneal irregularity under the projection of the placid rings. The corneal reflection circles were clear in the control group; however, the morphology of the reflection ring on the cornea of rats exposed to PM was irregular (Fig. 2A right-hand images). In the high-level PM-treated group, most of the cornea showed severe distortion

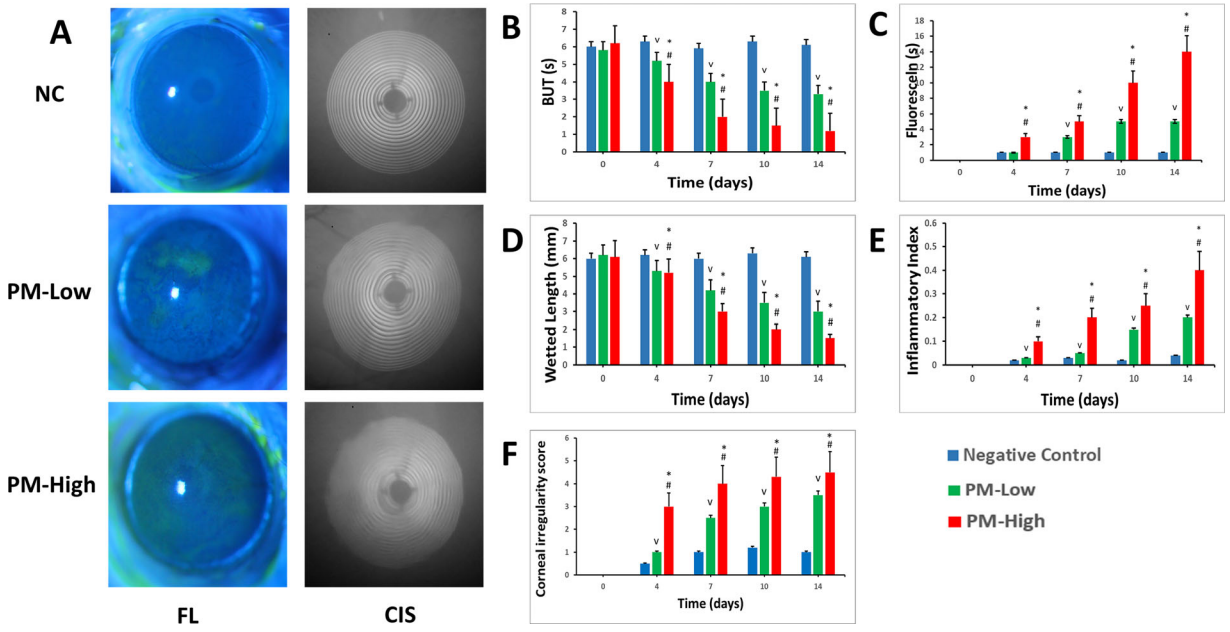

Figure 2. Alterations of the ocular surface, tear film stability, and degrees of inflammation after PM treatment. (**A**) Representative examples for day 14 of fluorescein sodium and corneal irregularity score (CIS) in PM-treated groups (the *lower panel*, high-level PM; the *middle panel*, low-level PM), compared with the control group (the *upper panel*). Increased corneal fluorescein staining scores and decreased BUTs of the ocular surface were recorded in the PM-treated groups at all time points ($P < 0.05$, respectively, **B, C**). Compared with the control group, the phenol red thread test showed markedly decreased tear volume production in the PM-treated groups for 14 days of treatment (**D**). (**E, F**) Increased corneal inflammatory index and corneal irregularity score after PM treatment. Each value represents the mean ± SD, $n = 10$. $^{*}P < 0.05$ PM-high versus control, $^{\#}P < 0.05$ PM-high versus PM-low, $^{v}P < 0.05$ PM-low versus control.

Investigative Ophthalmology & Visual Science

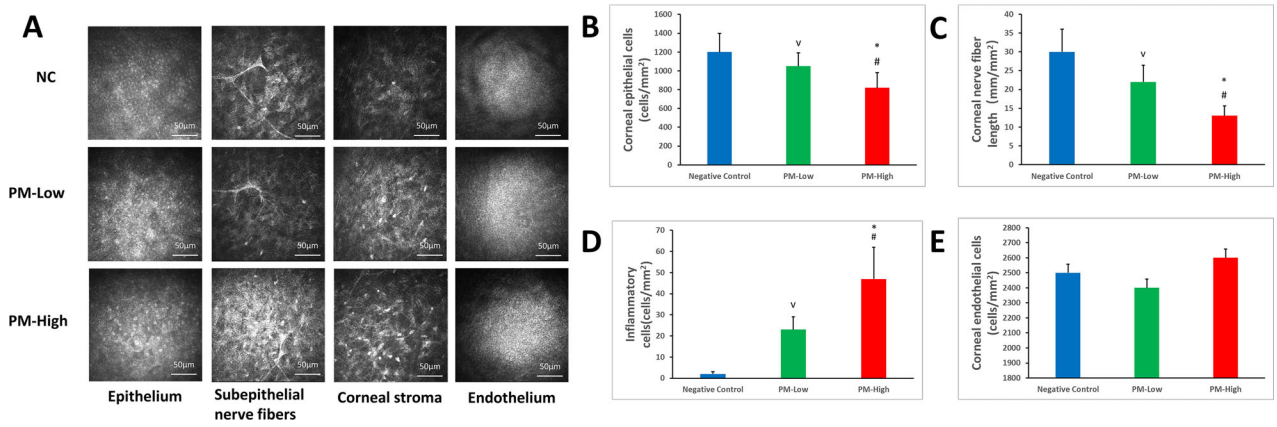

Figure 3. Examination of corneal confocal microscopy. (**A**) Representative examples for day 14 of corneal epithelial cells, subepithelial nerve fibers, corneal stroma, and corneal endothelial cells in PM-treated groups (**A**, the *lower line*, high-level PM and the *middle line*, low-level PM), compared with the control group (**A**, the *upper line*). Scale bar: 50 µm. (**B**) The mean of corneal epithelial cells density decreased significantly after PM treatment. (**C**) Corneal nerve fiber length was significantly decreased in the PM-treated group compared with the control group. (**D**) Increased corneal inflammatory cells infiltration after PM treatment. (**E**) There was no significant difference in the number of corneal endothelial cells in each group. Each value represents the mean ± SD, $n = 10$. $^{*}P < 0.05$ PM-high versus control, $^{\#}P < 0.05$ PM-high versus PM-low, $^{\text{v}}P < 0.05$ PM-low versus control.

reflection circles, in which even no ring could be recognized. The score of corneal irregularity increased significantly in the PM-exposed group, from 0.8 ± 0.2 (control group) to 3.2 ± 0.3 (low-level PM-treated group) and 4.3 ± 0.5 (high-level PM-treated group; $^{*}P < 0.05$ PM-high versus control, $^{\#}P < 0.05$ PM-high versus pm-low, $^{\text{v}}P < 0.05$ PM-low versus control; Fig. 2F).

Before treatment, there were no significant differences in BUT and fluorescein staining scores among the three groups. BUT was significantly decreased in PM-treated groups compared to control group (Fig. 2B), whereas the fluorescein sodium score (see Fig. 2A left-hand images and 2C) was significantly increased after day 4, day 7, day 10, and day 14, respectively ($P < 0.05$). After 14 days of treatment, corneal fluorescein sodium staining remained negative in control rats, whereas BUT and tear film / corneal damage scores were slightly changed, without significantly (see Figs. 2B, 2C). The damage of tear film / epithelial cells in the PM treatment group was concentration dependent and time-dependent, which may be related to the toxicity of PM. In addition, the BUT of high-level PM treated group was significantly lower than that of low-level group, whereas fluorescein staining score was significantly increased, respectively ($P < 0.05$).

The corneal confocal microscope can provide information on the changes in the structure of the cornea at the cellular level. The results showed that compared with the control group, the PM-treated rats showed a decrease in the number of corneal epithelial cells and an increase in volume, which was very similar to the corneal confocal image of a human dry eye. It is suggested that PM treatment appeared to induce not only functional changes to the rats to develop dry eye, but also morphological changes in epithelial cells. Corneal confocal microscopy did not reveal abnormalities in the corneal endothelium of the PM treated rats (Figs. 3A, 3B, 3E).

Aqueous Tear Volume

The phenol red thread tear test was used to measure aqueous tear volume. On day 0, there was no significant difference between the control group and the two PM-treated groups. After 4 days of treatment, compared with the control group, the tear volume of PM groups decreased faster ($P < 0.05$; see Fig. 2D), and from that day, the aqueous tear volume decrease of high-level PM-treated group was more obvious compared to the low-level group ($P < 0.05$; see Fig. 2D).

Inflammation Index and Cell Infiltration

There was a significant increase of inflammatory index at all time points in the PM-treated group compared to the control group, and the high-level PM-treated group also showed a higher level of inflammation index ($P < 0.05$; see Fig. 2E). In addition, the results of confocal microscopy and immunohistochemistry of inflammatory cells indicated that the PM-treated group showed more infiltration of inflammatory cells in the central cornea and conjunctiva compared with the control group ($P < 0.05$; see Figs. 3A, 3D, Fig. 4). The number of epithelial layers was significantly increased in the PM-treated eyes than in the control eyes in the central cornea after 14 days of treatment ($P < 0.05$; Figs. 5A, 5B).

Changes in Corneal Nerves

Confocal microscopy was used to examine corneal nerve alterations. The results showed a significant decrease in CNFL in the PM-treated groups compared with the control group on day 14, and the decrease was more pronounced in the high concentration group than in the low concentration group ($P < 0.05$; see Figs. 3A, 3C), accompanied by inflammatory cell infiltration, suggesting that PM can cause corneal nerve damage.

Goblet Cells Density

We examined the effects of PM treatment on corneal and conjunctival goblet cells with PAS staining. No PAS-positive cells were detected in the cornea in all groups (data not shown). The PAS-positive cell number was significantly

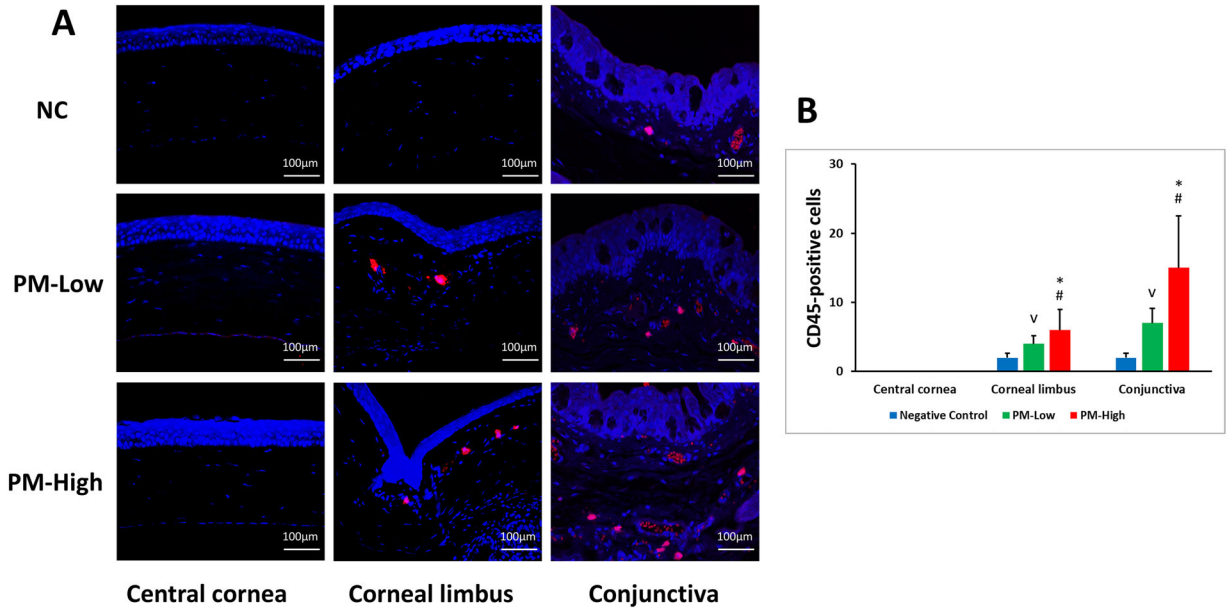

Figure 4. Inflammatory cell infiltration in corneal and conjunctival tissues in the control group and PM-treated groups. (**A**) Representative images for CD45 immunofluorescent staining of the corneal, limbus, and conjunctival epithelium/stroma on day 14. Scale bar: 100 μm. There was almost no infiltration of CD45-positive cells in the central corneal tissues of the control group and the PM-treated groups, whereas a few positive cells were found in the limbus, and the numbers in the PM-treated groups increased significantly. Compared with the control group, a significantly increase in CD45-positive cells was observed in the conjunctiva of the PM-treated groups after 14 days of treatment (**B**). Each value represents the mean ± SD, $n = 5$. $^{*}P < 0.05$ PM-high versus control, $^{\#}P < 0.05$ PM-high versus PM-low, $^{\text{v}}P < 0.05$ PM-low versus control.

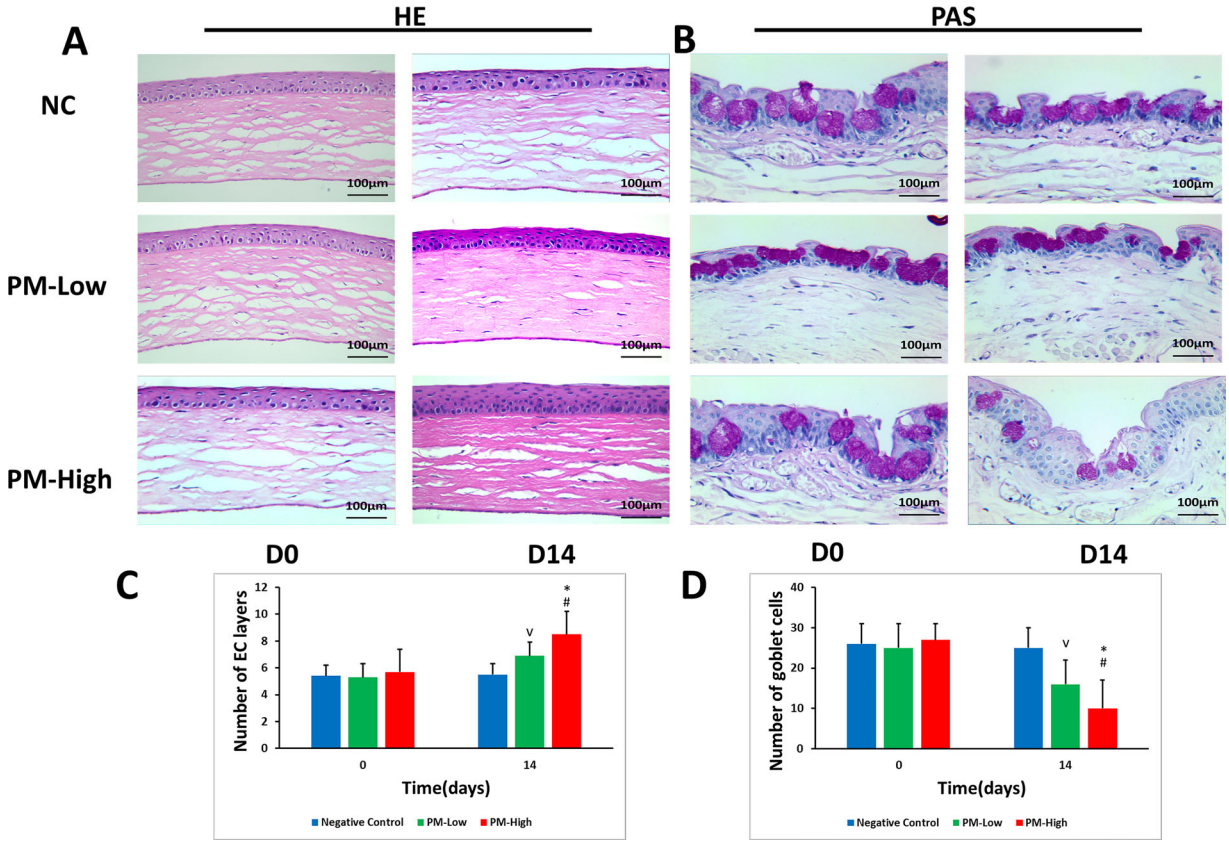

Figure 5. Alterations of the epithelial cells and goblet cells after PM treatment. (**A**, *left-hand images*) Representative images of H&E staining showing in the central cornea more layers of epithelium were observed in PM-treated eyes (the *lower panel*, high-level PM and the *middle panel*, low-level PM) than in the control group (the *upper panel*). (**A**, *right-hand images*) Representative images of PAS staining of the conjunctiva showed that, after 14 days of treatment, the goblet cells were abundantly present in the conjunctival fornix of the control eyes but significantly reduced in PM-treated groups. Scale bar: 100 μm. Statistical analysis of the epithelial cells (**B**) and goblet cells (**C**) of the three groups suggested no difference at day 0 but a markedly changes at day 14. Each value represents the mean ± SD, $n = 5$. $^{*}P < 0.05$ PM-high versus control, $^{\#}P < 0.05$ PM-high versus PM-low, $^{\text{v}}P < 0.05$ PM-low versus control.

Investigative Ophthalmology & Visual Science

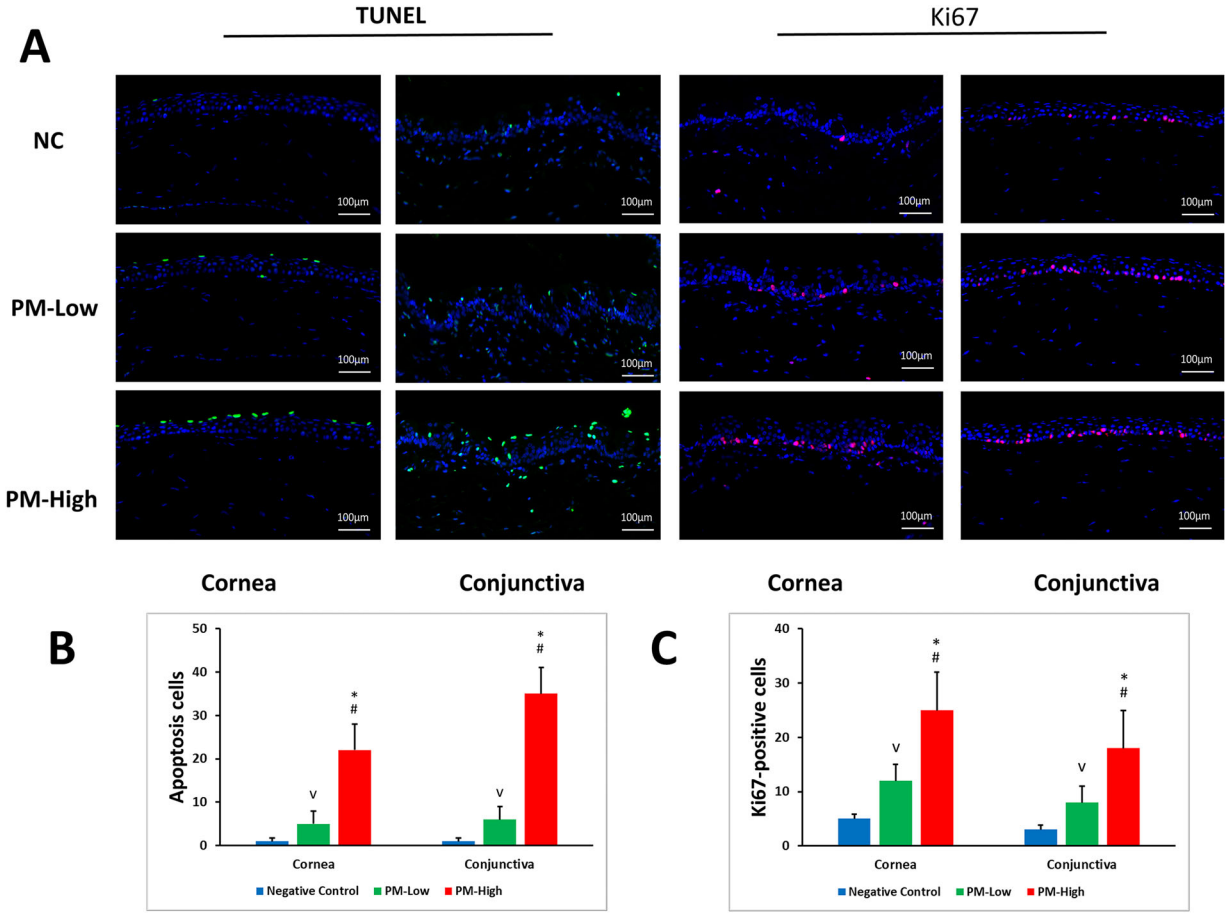

Figure 6. Corneal and conjunctival epithelial cell apoptosis and proliferation in the control group and PM-treated groups. Representative images for the TUNEL assay of the corneal epithelium and conjunctival epithelium on day 14 (**A**, *left-hand images*). Only a few apoptotic cells were observed in the superficial layer of the corneal and conjunctival epithelium in the control groups, whereas much more apoptosis was recorded in corneal and conjunctival superficial and basal epithelium after PM treatment (**B**). Representative images for Ki67 immunofluorescent staining of the corneal and conjunctival epithelium on day 14 (**A**, *right-hand images*). Ki67-positive cells were mainly located at the basal cell layer of corneal and conjunctival epithelium. Compared with the control group, a significantly increase in Ki67-positive cells was observed in both the central cornea and conjunctiva of the PM-treated groups after 14 days of treatment (**C**). Each value represents the mean ± SD, $n = 5$. $^{*}P < 0.05$ PM-high versus control, $^{\#}P < 0.05$ PM-high versus PM-low, $^{\text{v}}P < 0.05$ PM-low versus control.

decreased in both PM-treated groups, especially in the high-level PM-treated group, and the size of goblet cells seems to be smaller, whereas in the control group, the number of goblet cells had no significant change before and after treatment ($P < 0.05$; see Fig. 5A, right-hand images and 5C).

Apoptosis and Cell Proliferation

TUNEL assay showed that apoptosis was induced in the corneal superficial and basal epithelium, but not in the stroma in the PM-treated group. At the same time, there were apoptotic cells in conjunctival epithelium and superficial stroma, and the apoptotic cells in high-level PM-treated group increased significantly, whereas no apoptotic cells were observed in the corneal and conjunctival epithelium of the control group ($P < 0.05$; Fig. 6A left-hand images and 6B). Compared with the control group, the immunostaining of Ki67 revealed a drastic increase in Ki67-positive cells in both the central cornea and conjunctiva of the PM-groups after 14 days of treatment ($P < 0.05$; see Fig. 6A right-hand images and 6C), and Ki67-positive cells were mainly located at the basal cell layer of the cornea and conjunctiva.

Corneal Epithelial Ultrastructural Changes

Normal corneal epithelial cells have numerous well-arranged microvilli and outward extending microfolds that are essential for the maintenance of tear film stability. TEM showed that there were well-arranged microvilli and mitochondria/desmosomes in the corneal epithelial cells of the control group. In contrast, the number of microvilli and mitochondria/desmosomes in the corneal epithelium was significantly reduced in the PM-treated rats, especially in the high-level PM-treated group, and the microvilli morphology was also very different from that in the control group, with most of the microvilli being shorter and more disorganized ($P < 0.05$; Fig. 7).

Inflammatory Factors Change in the Ocular Surface

To investigate the pathogenesis of PM-induced dry eye, we analyzed the protein expression differences of NF-κB, IL-1β, and TNF-α by Western blotting among the three groups. The results revealed that compared to the control group, IL-1β and TNF-α protein levels were significantly

Investigative Ophthalmology & Visual Science

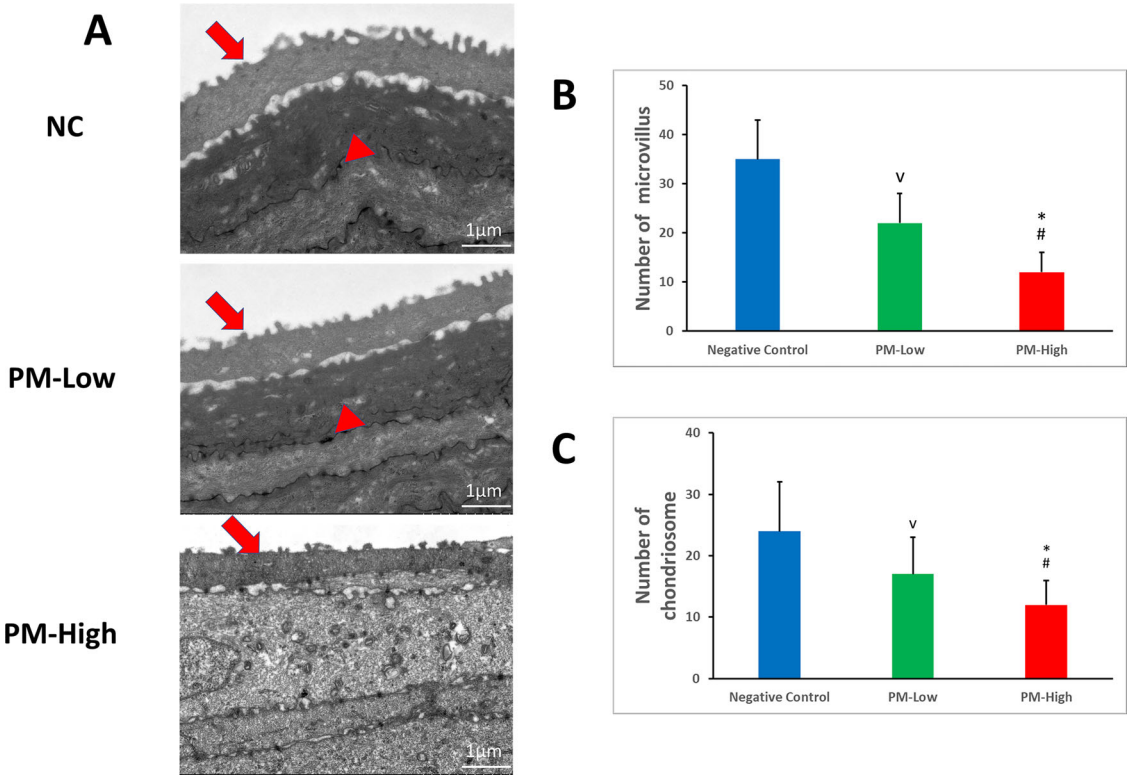

Figure 7. Transmission electron microscopy (TEM) images showing the ultrastructure of the corneal epithelium in the negative control group and PM-treated groups on day 14. Scale bar: 1 μm. In NC rats, epithelial microvilli (**A**, *red arrow head*) were extended digitately and arranged neatly (**A**, the *upper panel*). By contrast, the disordered corneal epithelial microvilli (**A**, *red arrow head*) were observed in PM-treated groups (**A**, the *lower panel*, high-level PM and the *middle panel*, low-level PM). Only a few microvilli (**B**) and chondriosome/desmosomes (**C**) were observed in the superficial layer of corneal epithelium in the PM-treated groups, whereas much more microvilli and chondriosome/desmosomes (**A**, *red arrows*) were recorded in corneal epithelium in control group. Each value represents the mean ± SD, $n = 5$. $^{*}P < 0.05$ PM-high versus control, $^{\#}P < 0.05$ PM-high versus PM-low, $^{v}P < 0.05$ PM-low versus control.

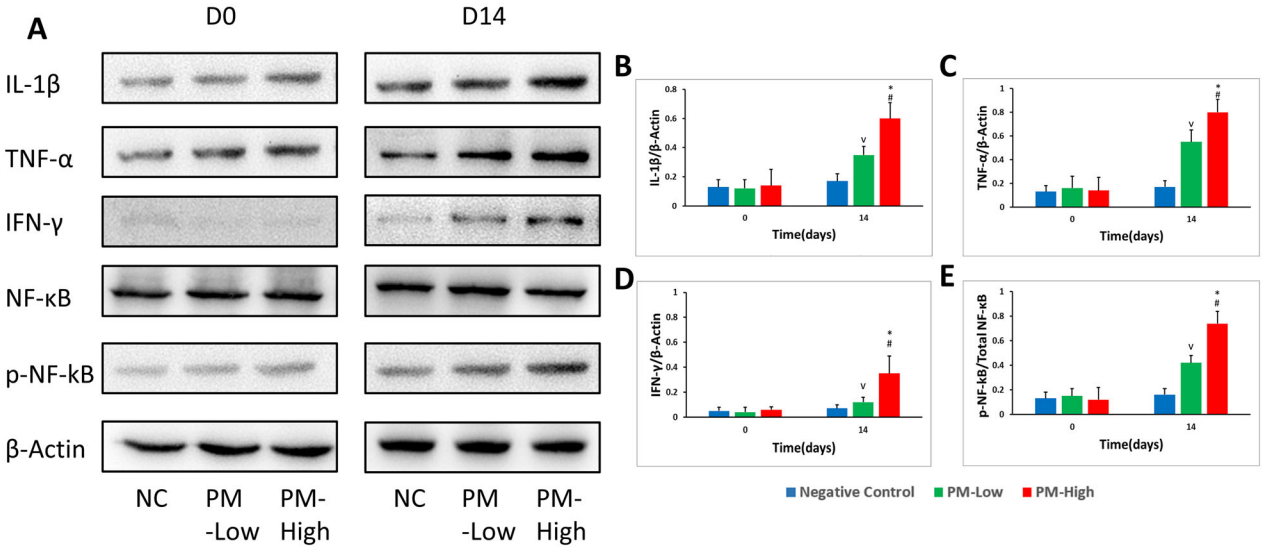

Figure 8. Effect of PM on IL-1β, TNF-α, IFN-γ, and NF-κB activation in the corneas evaluated by Western blot analysis, with β-Actin as a loading control. After treatment for 14 days, the protein level of IL-1β (**A**, the *first line*), TNF-α (**A**, the *second line*), and IFN-γ (**A**, the *third line*) in the PM cornea was upregulated and significantly higher than that in the NC group. (**B, C, D**) Statistical analysis of the band intensity values. Compared with the NC group, PM significantly increased the phosphorylation of NF-κB (**A**, the *fourth and fifth lines*). (**E**) Statistical analysis of the band intensity values. Data were presented as the mean + the SD, $n = 5$. $^{*}P < 0.05$ PM-high versus control, $^{\#}P < 0.05$ PM-high versus PM-low, $^{v}P < 0.05$ PM-low versus control.

Investigative Ophthalmology & Visual Science

higher in PM-treated ocular surface, especially in the high-level PM treated group. Compared with the control group, phosphorylated-NF-κB was significantly increased in PM-treated group, whereas the expression of NF-κB was in the same level ($P < 0.05$; Fig. 8). Taken together, these data suggest that aerosol PM activates inflammatory responses on the ocular surface and that activation of the NF-κB signaling pathway may play an important role in the development of dry eye.

Discussion

PM, as one of the main components of atmospheric pollutants, has aroused widespread concern with regard to its impact on health.[43,44] In recent years, air pollution has become one of the biggest social problems in China, and PM levels have reached "bad" or "very bad" levels in many large cities according to the standards defined by the WHO air quality guidelines.[45] Establishing suitable animal models with PM exposure levels as close as possible to actual atmospheric PM is essential for studying the association of PM with human diseases, as well as the associated pathogenesis and clinical treatment. Aerosol exposure systems are widely used to assess the effects of inhaled air pollutants, such as PM and cigarette smoke, etc.,[46] on the respiratory and circulatory systems, which are simple and stable in structure and can establish environmental conditions similar to ambient air pollution around urban areas, so, in this study, we utilized this system to evaluate the effects of PM on the eyes.

Dry eye has been defined by TFOS DEW II as "a multifactorial disease of the ocular surface characterized by a loss of homeostasis of the tear film, and accompanied by ocular symptoms" in 2017.[1] As physical contact (e.g. wearing contact lens) with the eyes could have an impact on DES development,[47] contact of air pollutants may have similar effects. Because air pollution has been confirmed to be associated with allergic conjunctivitis,[48,49] as one of the organs exposed to the environment directly, the ocular surface also suffers from PM, and it is of interest to determine whether air pollution is also related to dry eye. In the literature review, some clinical studies showed a significant relationship between air pollution and dry eye, albeit with inconsistent air pollutants.[18,50,51] In animal models of dry eye, topical instillation of PM can lead to decreased tear secretion, damage to the corneal and conjunctival epithelia, reduced numbers of goblet cells, and altered ocular surface microenvironment, exhibiting structural and functional characteristics similar to human dry eye.[24,25] However, a large amount of PM was exposed in a short time using the PM topical eye drops method, which is incompatible with the practical environment. Moreover, Friedlaender et al.[52] have reported that the concentration of substances in eye drops dilutes 8 times in 30 seconds, 16 times in 1 minute, and 36 times in 2 minutes because of a tear when topical medication is applied to the eyes, therefore, it is not an ideal model to observe PM effect on ocular surface by local administration as eye drop. In our experiment, the air pollution in the natural environment is simulated by the way of PM atomization and resuspension, the model is closer to the real level, and the concentration of PM can be measured accurately, as a result the experimental data are more reliable. Furthermore, we set the low concentration group and high concentration group of PMs, so we can observe the effect of different PM concentration on the stability of tear film.

As we all know, there is an inflammatory vicious cycle in dry eye,[53] inflammation is often the primary cause and consequence of reduced stability and dryness of the ocular surface, and inflammatory cell infiltration, inflammatory factor release can lead to epithelial cell apoptosis, abnormal epithelial cell proliferation, decreased goblet cell numbers, keratoconjunctival metaplasia, and squamous metaplasia.[54] By confocal microscopy and CD45 immunohistochemical staining, we confirmed that the PM-induced rat dry eye was combined with inflammatory cell infiltration. Under the feedback of inflammatory activation, compared with the control group, the PM-treated group exhibited significantly decreased tear production, higher ocular staining scores, and lower goblet cell density, suggesting that the PM-treated group developed significant ocular surface damage.

From the analysis of experimental data, we found that after PM treatment, the tear volume, BUT, corneal fluorescein staining, and corneal irregularity score of the experimental group were significantly reduced, but the control group had no significant change, indicating that the PM-treated group presented the dry eye characteristic decreased tear film stability. The corneal and conjunctival epithelia are fundamental structures of the ocular surface and important barriers against invasion by pathogens.[55] Damage to the corneal and conjunctival epithelium is one of the characteristic features of dry eye disease progression. In such injuries, epithelial apoptosis is often observed.[56,57] TUNEL assay showed that the apoptosis of corneal and conjunctival epithelial cells was significantly increased in the experimental group after PM treatment, which suggested that this PM aerosol exposure system caused corneal and conjunctival epithelial damage. As a compensation procedure for injury repair, compared with the control group, the keratocytes in the PM-treated group can observe the obvious cell proliferation, which is usually pathological with inflammatory response.

The H&E staining and electron microscopy revealed that the epithelial cell layer was thickened, and the corneal surface planarity was reduced, with irregular epithelial cell morphology, shorter and disorganized corneal epithelial microvilli, and reduced intercellular desmosome junctions in the PM-treated rats. These results indicated that PM exposure could cause damage to corneal epithelial cells, which were mutually verified with the above clinical index detection results and TUNEL assay. However, it is still an unsolved problem whether PM directly causes corneal epithelial injury or through inflammatory reaction and apoptosis. Among the chemical induced ocular surface damage models, the benzalkonium chloride (BAK) topical eye drops induced dry eye model has been widely recognized.[58] The composition of PM is complex, in which water-soluble inorganic salts and carbonaceous components are the main components, and we found that the phenotype of the PM-induced dry eye model was very similar to the BAK-induced dry eye model. Which component of PM plays the most important role in inducing dry eyes is also an interesting research topic in the future.

Studies have shown that proinflammatory cytokines may play a key role in the pathogenesis of a variety of corneal diseases, including dry eye.[59] Pflugfelder et al.[60] were the first to show increased levels of proinflammatory cytokines in tear fluid from patients with dry eye, and they also demonstrated a strong correlation between tear cytokine levels and clinical indicators associated with dry eye.[61] Villani

Investigative Ophthalmology & Visual Science

et al.[62] analyzed the correlation between corneal dendritic cell density and tear inflammatory cytokines in patients with rheumatoid arthritis (RA)-associated dry eye and found that IL-1 and IL-6 concentrations decreased after systemic treatment for RA, as did corneal dendritic cell density by confocal microscopy. Other studies reported that topical treatment with steroid eye drops[63] or intense pulsed light therapy[64] in patients with meibomian gland dysfunction (MGD) was effective in reducing tear cytokine levels. Cytokine IL-1β and TNF-α were produced by epithelial cells and tissue infiltrating inflammatory cells under stress, and NF-κB signaling pathways were activated by phosphorylation under inflammatory conditions.[65] The results showed that PM exposure can activate IL-1β, NF-κB, and TNF-α, and the protein expression level increased in a dose-dependent manner. Whether inhibiting the expression of inflammatory factors, such as IL-1β and TNF-α, and activating the NF-κB signaling pathway can reduce the inflammation level of dry eye is an interesting research direction in the future. Dry eye is a chronic disease with multiple factors, and further research is needed to understand the mechanism of PM-induced dry eye. Because inflammation is crucial in the pathogenesis of dry eye, anti-inflammatory drugs may be good candidates for the treatment of dry eye. The dry eye model of rats induced by PM exposure can be used to evaluate the therapeutic effects of these drugs. In addition to inflammatory reaction, the pathogenesis of dry eye also includes oxidative stress, autophagy, and so on. Evidence has shown that the PM-induced dry eye model has apoptosis of keratoconjunctival epithelial cells, but whether this apoptosis is the result of inflammation or an independent cause is not clear. Whether other pathogenesis are involved in the PM-induced dry eye model also needs further study.

Mucin plays an important role in maintaining the stability of the tear film. The goblet cells of the conjunctiva secrete the mucin component MUC5AC in the tear film. The number of goblet cells decrease after inflammation or injury of the ocular surface, which is considered to be sensitive to ocular surface damage. Compared with the control group, the mucin-positive goblet cells in the PM-treatment group were significantly reduced, and this decrease was more obvious in the high concentration group. The mechanism of ocular surface damage caused by air pollution is not yet clear. Through in vitro experiments, some studies have confirmed the effect of air pollutants on the ocular surface, such as increased expression of inflammatory cytokines, increased damage and apoptosis of corneal and conjunctival epithelial cells, and decreased goblet cells.[66,67] Our results were consistent with these experimental changes. The reason for the decrease of goblet cells induced by PM is not clear, which may be related to the direct toxic effect of PM, and may also be related to the secondary immune response and apoptosis. Furthermore, whether the decline of goblet cells can recover after being separated from the PM environment remains to be further studied.

In conclusion, our animal experiment results show that aerosol PM will reduce the stability of the tear film, leading to changes in the ocular surface structure, and then forming a phenotype similar to human dry eye. In order to further study the mechanism of PM-induced ocular surface damage, we will explore whether it is related to the change of tear osmotic pressure or the decrease of mucin secretion, which leads to the increase of inflammatory factors in tears and the instability of the tear film. We will also examine whether PM can cause the pathological changes of corneal squamous epithelial metaplasia or corneal conjunctivalization, and damage the eyelid glands (including meibomian glands and lacrimal glands). At the same time, we will actively look for effective treatment drugs (such as anti-inflammatory drugs and drugs that promote mucin secretion) and preventive measures to reduce the damage of PM to the eyes.

Acknowledgments

Disclosure: **N. Mu,** None; **H. Wang,** None; **D. Chen,** None; **F. Wang,** None; **L. Ji,** None; **C. Zhang,** None; **M. Li,** None; **P. Lu,** None

References

1. Craig JP, Nichols KK, Akpek EK, et al. TFOS DEWS II Definition and Classification Report. *Ocul Surf*. 2017;15(3):276–283.
2. McMonnies CW. Measurement of Symptoms Pre- and Post-treatment of Dry Eye Syndromes. *Optom Vis Sci*. 2016;93(11):1431–1437.
3. Chen CH, Yang TY, Lin CL, et al. Dry Eye Syndrome Risks in Patients With Fibromyalgia: A National Retrospective Cohort Study. *Medicine (Baltimore)*. 2016;95(4):e2607.
4. Asiedu K, Kyei S, Boampong F, Ocansey S. Symptomatic Dry Eye and Its Associated Factors: A Study of University Undergraduate Students in Ghana. *Eye Contact Lens*. 2017;43(4):262–266.
5. Tesón M, López-Miguel A, Neves H, Calonge M, González-García MJ, González-Méijome JM. Influence of Climate on Clinical Diagnostic Dry Eye Tests: Pilot Study. *Optom Vis Sci*. 2015;92(9):e284–e289.
6. Sosne G, Kim C, Kleinman HK. Thymosin β4 significantly reduces the signs of dryness in a murine controlled adverse environment model of experimental dry eye. *Expert Opin Biol Ther*. 2015;15(Suppl 1):S155–S161.
7. Yang T. Association between perceived environmental pollution and health among urban and rural residents-a Chinese national study. *BMC Public Health*. 2020;20(1):194.
8. Landrigan PJ, Fuller R. Global health and environmental pollution. *Int J Public Health*. 2015;60(7):761–762.
9. Loxham M, Nieuwenhuijsen MJ. Health effects of particulate matter air pollution in underground railway systems - a critical review of the evidence. *Part Fibre Toxicol*. 2019;16(1):12.
10. Whyand T, Hurst JR, Beckles M, Caplin ME. Pollution and respiratory disease: can diet or supplements help? A review. *Respir Res*. 2018;19(1):79.
11. Mokoena KK, Ethan CJ, Yu Y, Shale K, Liu F. Ambient air pollution and respiratory mortality in Xi'an, China: a time-series analysis. *Respir Res*. 2019;20(1):139.
12. Piao MJ, Ahn MJ, Kang KA, et al. Particulate matter 2.5 damages skin cells by inducing oxidative stress, subcellular organelle dysfunction, and apoptosis. *Arch Toxicol*. 2018;92(6):2077–2091.
13. Hayes RB, Lim C, Zhang Y, et al. PM2.5 air pollution and cause-specific cardiovascular disease mortality. *Int J Epidemiol*. 2020;49(1):25–35.
14. Franklin BA, Brook R, Arden Pope C, 3rd. Air pollution and cardiovascular disease. *Curr Probl Cardiol*. 2015;40(5):207–238.
15. Eze IC, Hemkens LG, Bucher HC, et al. Association between ambient air pollution and diabetes mellitus in Europe and North America: systematic review and meta-analysis. *Environ Health Perspect*. 2015;123(5):381–389.
16. Darbre PD. Overview of air pollution and endocrine disorders. *Int J Gen Med*. 2018;11:191–207.
17. Yoon S, Han S, Jeon KJ, Kwon S. Effects of collected road dusts on cell viability, inflammatory response, and oxidative

stress in cultured human corneal epithelial cells. *Toxicol Lett*. 2018;284:152–160.
18. Mo Z, Fu Q, Lyu D, et al. Impacts of air pollution on dry eye disease among residents in Hangzhou, China: A case-crossover study. *Environ Pollut*. 2019;246:183–189.
19. Niu L, Li L, Xing C, et al. Airborne particulate matter (PM(2.5)) triggers cornea inflammation and pyroptosis via NLRP3 activation. *Ecotoxicol Environ Saf*. 2021;207:111306.
20. Fu Q, Lyu D, Zhang L, et al. Airborne particulate matter (PM2.5) triggers autophagy in human corneal epithelial cell line. *Environ Pollut*. 2017;227:314–322.
21. Kashiwagi K, Iizuka Y. Effect and underlying mechanisms of airborne particulate matter 2.5 (PM2.5) on cultured human corneal epithelial cells. *Sci Rep*. 2020;10(1):19516.
22. Yang Q, Tang L, Shen M, et al. Effects of diesel exhaust particles on the condition of mouse ocular surface. *Ecotoxicol Environ Saf*. 2018;163:585–593.
23. Tau J, Novaes P, Matsuda M, Tasat DR, Saldiva PH, Berra A. Diesel exhaust particles selectively induce both proinflammatory cytokines and mucin production in cornea and conjunctiva human cell lines. *Invest Ophthalmol Vis Sci*. 2013;54(7):4759–4765.
24. Li J, Tan G, Ding X, et al. A mouse dry eye model induced by topical administration of the air pollutant particulate matter 10. *Biomed Pharmacother*. 2017;96:524–534.
25. Tan G, Li J, Yang Q, et al. Air pollutant particulate matter 2.5 induces dry eye syndrome in mice. *Sci Rep*. 2018;8(1):17828.
26. Song SJ, Hyun SW, Lee TG, Park B, Jo K, Kim CS. New application for assessment of dry eye syndrome induced by particulate matter exposure. *Ecotoxicol Environ Saf*. 2020;205:111125.
27. Shen Z, Cao J, Liu S, et al. Chemical composition of PM10 and PM2.5 collected at ground level and 100 meters during a strong winter-time pollution episode in Xi'an, *China J Air Waste Manag Assoc*. 2011;61(11):1150–1159.
28. Larcombe AN, Janka MA, Mullins BJ, Berry LJ, Bredin A, Franklin PJ. The effects of electronic cigarette aerosol exposure on inflammation and lung function in mice. *Am J Physiol Lung Cell Mol Physiol*. 2017;313(1):L67–L79.
29. Guan L, Geng X, Stone C, et al. PM(2.5) exposure induces systemic inflammation and oxidative stress in an intracranial atherosclerosis rat model. *Environ Toxicol*. 2019;34(4):530–538.
30. Ward RX, Tilly TB, Mazhar SI, et al. Mimicking the human respiratory system: Online in vitro cell exposure for toxicity assessment of welding fume aerosol. *J Hazard Mater*. 2020;395:122687.
31. Krzyzanowski M. WHO Air Quality Guidelines for Europe. *J Toxicol Environ Health A*. 2008;71(1):47–50.
32. Yu D, Deng Q, Wang J, et al. Air Pollutants are associated with Dry Eye Disease in Urban Ophthalmic Outpatients: a Prevalence Study in China. *J Transl Med*. 2019;17(1):46.
33. Tao C, Tang Y, Zhang L, Tian Y, Zhang Y. Atomization method for verifying size effects of inhalable particles on lung damage of mice. *Sci Total Environ*. 2017;579:1476–1484.
34. Lemp MA. Report of the National Eye Institute/Industry workshop on Clinical Trials in Dry Eyes. *CLAO J*. 1995;21(4):221–232.
35. Xiao X, He H, Lin Z, et al. Therapeutic effects of epidermal growth factor on benzalkonium chloride-induced dry eye in a mouse model. *Invest Ophthalmol Vis Sci*. 2012;53(1):191–197.
36. Patel DV, McGhee CN. Quantitative analysis of in vivo confocal microscopy images: a review. *Surv Ophthalmol*. 2013;58(5):466–675.
37. Matsumoto Y, Ibrahim O. Application of In Vivo Confocal Microscopy in Dry Eye Disease. *Invest Ophthalmol Vis Sci*. 2018;59(14):DES41–DES47.
38. Xiao X, Luo P, Zhao H, et al. Amniotic membrane extract ameliorates benzalkonium chloride-induced dry eye in a murine model. *Exp Eye Res*. 2013;115:31–40.
39. Zhang Z, Yang WZ, Zhu ZZ, et al. Therapeutic effects of topical doxycycline in a benzalkonium chloride-induced mouse dry eye model. *Invest Ophthalmol Vis Sci*. 2014;55(5):2963–2974.
40. Williams KA, Standfield SD, Smith JR, Coster DJ. Corneal graft rejection occurs despite Fas ligand expression and apoptosis of infiltrating cells. *Br J Ophthalmol*. 2005;89(5):632–638.
41. Stephens DN, McNamara NA. Altered Mucin and Glycoprotein Expression in Dry Eye Disease. *Optom Vis Sci*. 2015;92(9):931–938.
42. Li C, Song Y, Luan S, et al. Research on the stability of a rabbit dry eye model induced by topical application of the preservative benzalkonium chloride. *PLoS One*. 2012;7(3):e33688.
43. Orru H, Ebi KL, Forsberg B. The Interplay of Climate Change and Air Pollution on Health. *Curr Environ Health Rep*. 2017;4(4):504–513.
44. Kim KH, Kabir E, Kabir S. A review on the human health impact of airborne particulate matter. *Environ Int*. 2015;74:136–143.
45. Fang W, Song W, Liu L, et al. Characteristics of indoor and outdoor fine particles in heating period at urban, suburban, and rural sites in Harbin, *China Environ Sci Pollut Res Int*. 2020;27(2):1825–1834.
46. Kant N, Müller R, Braun M, Gerber A, Groneberg D. Particulate Matter in Second-Hand Smoke Emitted from Different Cigarette Sizes and Types of the Brand Vogue Mainly Smoked by Women. *Int J Environ Res Public Health*. 2016;13(8):799.
47. Kojima T. Contact Lens-Associated Dry Eye Disease: Recent Advances Worldwide and in Japan. *Invest Ophthalmol Vis Sci*. 2018;59(14):DES102–DES108.
48. Chen R, Yang J, Zhang C, et al. Global Associations of Air Pollution and Conjunctivitis Diseases: A Systematic Review and Meta-Analysis. *Int J Environ Res Public Health*. 2019;16(19):3652.
49. Chen R, Yang J, Chen D, et al. Air pollution and hospital outpatient visits for conjunctivitis: a time-series analysis in Tai'an, *China*. *Environ Sci Pollut Res Int*. 2021;28(12):15453–15461.
50. Mandell JT, Idarraga M, Kumar N, Galor A. Impact of Air Pollution and Weather on Dry Eye. *J Clin Med*. 2020;9(11):3740.
51. Zhong JY, Lee YC, Hsieh CJ, Tseng CC, Yiin LM. Association between Dry Eye Disease, Air Pollution and Weather Changes in Taiwan. *Int J Environ Res Public Health*. 2018;15(10):2269.
52. Friedlaender MH, Breshears D, Amoozgar B, Sheardown H, Senchyna M. The dilution of benzalkonium chloride (BAK) in the tear film. *Adv Ther*. 2006;23(6):835–841.
53. Yamaguchi T. Inflammatory Response in Dry Eye. *Invest Ophthalmol Vis Sci*. 2018;59(14):DES192–DES199.
54. Dartt DA, Masli S. Conjunctival epithelial and goblet cell function in chronic inflammation and ocular allergic inflammation. *Curr Opin Allergy Clin Immunol*. 2014;14(5):464–470.
55. Meloni M, De Servi B, Marasco D, Del Prete S. Molecular mechanism of ocular surface damage: application to an in vitro dry eye model on human corneal epithelium. *Mol Vis*. 2011;17:113–126.

Investigative Ophthalmology & Visual Science

56. Seo Y, Ji YW, Lee SM, et al. Activation of HIF-1α (hypoxia inducible factor-1α) prevents dry eye-induced acinar cell death in the lacrimal gland. *Cell Death Dis*. 2014;5(6):e1309.
57. Lai CT, Yao WC, Lin SY, et al. Changes of Ocular Surface and the Inflammatory Response in a Rabbit Model of Short-Term Exposure Keratopathy. *PLoS One*. 2015;10(9):e0137186.
58. Lin Z, Liu X, Zhou T, et al. A mouse dry eye model induced by topical administration of benzalkonium chloride. *Mol Vis*. 2011;17:257–264.
59. Nicolle P, Liang H, Reboussin E, et al. Proinflammatory Markers, Chemokines, and Enkephalin in Patients Suffering from Dry Eye Disease. *Int J Mol Sci*. 2018;19(4):1221.
60. Pflugfelder SC, Jones D, Ji Z, Afonso A, Monroy D. Altered cytokine balance in the tear fluid and conjunctiva of patients with Sjögren's syndrome keratoconjunctivitis sicca. *Curr Eye Res*. 1999;19(3):201–211.
61. Luo L, Li DQ, Corrales RM, Pflugfelder SC. Hyperosmolar saline is a proinflammatory stress on the mouse ocular surface. *Eye Contact Lens*. 2005;31(5):186–193.
62. Villani E, Galimberti D, Del Papa N, Nucci P, Ratiglia R. Inflammation in dry eye associated with rheumatoid arthritis: cytokine and in vivo confocal microscopy study. *Innate Immun*. 2013;19(4):420–427.
63. Lee H, Chung B, Kim KS, Seo KY, Choi BJ, Kim TI. Effects of topical loteprednol etabonate on tear cytokines and clinical outcomes in moderate and severe meibomian gland dysfunction: randomized clinical trial. *Am J Ophthalmol*. 2014;158(6):1172–1183.e1.
64. Liu R, Rong B, Tu P, et al. Analysis of Cytokine Levels in Tears and Clinical Correlations After Intense Pulsed Light Treating Meibomian Gland Dysfunction. *Am J Ophthalmol*. 2017;183:81–90.
65. Roda M, Corazza I, Bacchi Reggiani ML, et al. Dry Eye Disease and Tear Cytokine Levels-A Meta-Analysis. *Int J Mol Sci*. 2020;21(9):3111.
66. Torricelli AA, Matsuda M, Novaes P, et al. Effects of ambient levels of traffic-derived air pollution on the ocular surface: analysis of symptoms, conjunctival goblet cell count and mucin 5AC gene expression. *Environ Res*. 2014;131:59–63.
67. Fujishima H, Satake Y, Okada N, Kawashima S, Matsumoto K, Saito H. Effects of diesel exhaust particles on primary cultured healthy human conjunctival epithelium. *Ann Allergy Asthma Immunol*. 2013;110(1):39–43.